Communications in Applied Analysis **10** (2006), no. 4, 531–550

ON SOLVING A SET OF NONLINEAR EQUATIONS FOR THE DETERMINATION OF STRESSES IN RC RING SECTIONS WITH OPENINGS

Andrzej Stachurski[1] and Marek Lechman[2]

[1]Institute of Control and Computation Engineering
Warsaw University of Technology
Nowowiejska 15/19, Warsaw, 00-665, Poland
A.Stachurski@ia.pw.edu.pl

[2]Building Research Institute
Filtrowa 1, Warsaw, 00-611, Poland
m.lechman@itb.pl

Communicated by D. Bainov

ABSTRACT: The paper deals with the analytical model for the normal stresses in the reinforced concrete (RC) ring cross sections weakened by openings. The aim of the paper is to compare numerically the least squares approach with a direct method for solving sets of nonlinear equations forming the model.

In the least squares approach the resulting optimization problem is to minimize the sums of the second powers of the residuals of the equations. The feasible points area is represented by the box constraints following from the physical sense of the variables. The resulting minimization problems are solved by means of the BFGS quasi-Newton and/or Hooke-Jeeves local minimizers suitably modified to take into account the box constraints.

The Broyden quasi-Newton method was implemented and tested in the direct approach to solve the sets of nonlinear equations. It uses an approximation of the Jacobi matrix inverse at each iteration to generate the consecutive point.

AMS (MOS) Subject Classification: 74B20, 74C15, 74S30

Received August 24, 2006

1. INTRODUCTION

Determination of the normal strains and stresses in RC ring cross sections weakened by openings due to the normal force and the bending moment has been analysed as a theoretical problem as well as a practical one. Such cross sections are encountered in structural design (tower structures, chimneys, pipes, etc.), see Lechman and Stachurski [8]. In the paper, the governing equations for the normal strains and stresses due to the bending moment and the normal force are derived for the case when openings are located symmetrically in respect to the bending direction.

The resulting sets of nonlinear equations are solved in two ways either directly by means of the Broyden quasi-Newton method or using the least squares approach where the sums of the second powers of the equations residuals are minimized. The second approach requires the use of the optimization techniques. The solution is searched by means of the modified BFGS and Hooke-Jeeves methods (see Bazaraa et al [1], Bertsekas [2], Broyden [3] and Broyden [4], Fletcher [5], Stachurski and Wierzbicki [9]). Both presented approaches enable the evaluation of the strains and stresses in the ring cross sections by the interactive analysis.

For presentation of the proposed section model the annular cross section weakened by one opening is chosen.

2. DERIVATION OF EQUATIONS FOR THE SECTION WITH ONE OR TWO OPENINGS

The annular cross-section, described by the outer radius – R and the inter radius – r, is assumed to be weakened by one or two openings. The locations of openings are determined by couples of the angular coordinates $(0, \alpha_1)$ and (α_2, π), $0 \leq \alpha_1 \leq \alpha_2 \leq \pi$. The reinforcing steel spaced in a general case continuously at l layers can be replaced by a continuous ring of equivalent area located on the reference circumference of radius r_s. The section under consideration is subject to the normal force N and the bending moment M.

In the present derivation the following assumptions are introduced:

(1) the distribution of strain across the section is plane,
(2) the tensile strength of concrete is ignored,
(3) the reinforcement in both the tension and compression zone is taken into account,
(4) the shell is thin compared with its diameter,
(5) elasto-plastic stress/strain relationships for concrete and steel are used,
(6) the ultimate strain for concrete is defined as - 0.0035, while for reinforcement as 0.005 (tension) and -0.005 (compression).

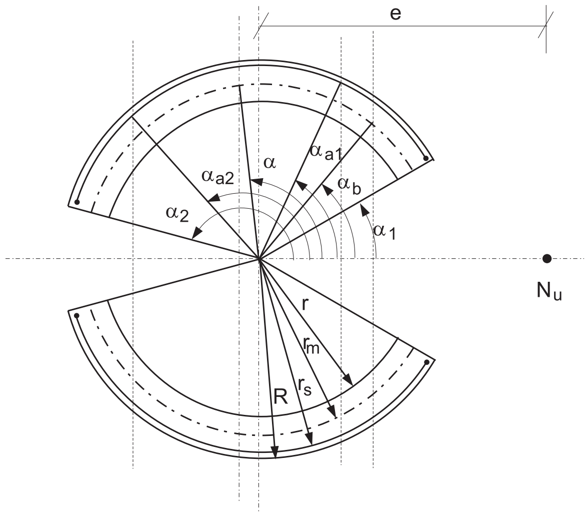

Figure 1. The cross-section weakened by two openings

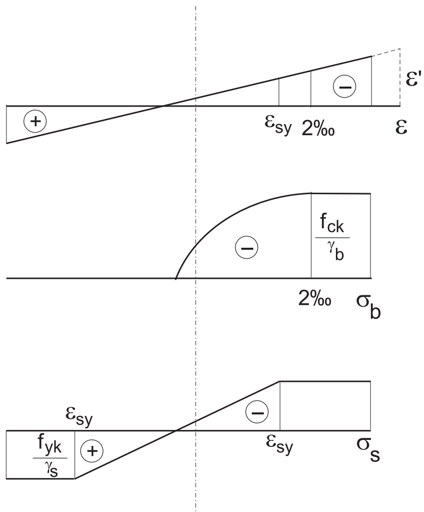

Figure 2. Distribution of strains ϵ, stresses in concrete σ_b and in steel σ_s across the section

The stress-strain relationships for concrete in compression are assumed as (Figure 1 and Figure 2):

$$\begin{aligned} \sigma_b &= \frac{f_{ck}}{\gamma_c}\,\epsilon\,(1+0.25\epsilon)\,, \qquad -2 \le \epsilon \le 0\,, \\ \sigma_b &= -\frac{f_{ck}}{\gamma_c}\,, \qquad -3.5 \le \epsilon \le -2\,, \end{aligned} \tag{1}$$

where: σ_b – compressive stress in concrete, ϵ – strain in concrete, expressed per mille, $[^o/_{oo}]$, f_{ck} – the characteristic strength of concrete in compression, γ_c – partial safety factor for concrete.

The material law for steel in tension and compression is given by (Figure 2):

$$\begin{aligned} \sigma_s &= \frac{f_{yk}}{\epsilon_s}\,\epsilon\,, && -\frac{\epsilon_s}{\gamma_s} \le \epsilon \le \frac{\epsilon_s}{\gamma_s}\,, \\ \epsilon_s &= \frac{f_{yk}}{E_s}\,, && \\ \sigma_s &= \frac{f_{yk}}{\gamma_s}\,, && \frac{\epsilon_s}{\gamma_s} \le \epsilon \le 5\,, \\ \sigma_s &= -\frac{f_{yk}}{\gamma_s}\,, && -5 \le \epsilon \le -\frac{\epsilon_s}{\gamma_s} \end{aligned} \tag{2}$$

where: f_{yk} – the yield stress of steel, γ_s – partial safety factor for steel, E_s – modulus of elasticity of steel.

Due to the Bernoulli assumption we obtain:

$$\begin{aligned} \epsilon_b &= \frac{\cos\varphi - \cos\alpha}{\rho_R - \cos\alpha}\,\dot{\epsilon}\,, \\ \epsilon_a &= \frac{\rho\cos\varphi - \cos\alpha}{\rho_R - \cos\alpha}\dot{\epsilon}\,, \end{aligned} \tag{3}$$

where: ϵ_b, ϵ_a – strains in concrete and steel, respectively, $\dot{\epsilon}$ – the maximum compressive strain in concrete, α – the angle describing the location of the neutral axis, φ – angular coordinate, r_m – mean radius of the ring (equal to the centroidal radius of concrete r_c), ρ – coefficient $\rho = r_s/r_m$, ρ_R – coefficient $\rho_R = R/r_m$.

The equilibrium equation of the normal forces in the cross-section weakened by one or two openings takes the following form:

$$\begin{aligned} &-\frac{1-\mu}{\gamma_c}(\alpha_b - \alpha_1) \\ &\quad + \frac{1-\mu}{\gamma_c}\frac{\dot{\epsilon}}{\rho_R - \cos\alpha}\left[X_1(\alpha,\alpha_b) + \frac{\dot{\epsilon}}{4(\rho_R - \cos\alpha)}X_2(\alpha,\alpha_b)\right] \\ &+ \mu\frac{f_{yk}}{f_{ck}}\left[-\frac{1}{\gamma_s}(\alpha_{a1} - \alpha_1) + \frac{1}{\epsilon_s}\frac{\dot{\epsilon}}{\rho_R - \cos\alpha}X_3(\alpha_{a1},\alpha_{a2}) + \frac{1}{\gamma_s}(\alpha_2 - \alpha_{a2})\right] \\ &\qquad + \frac{N}{2r_m t f_{ck}} = 0\,, \end{aligned} \tag{4}$$

where:

$$
\begin{aligned}
X_1(\alpha,\alpha_b) &= \sin\alpha - \sin\alpha_b - \cos\alpha(\alpha-\alpha_b)\,, \\
X_2(\alpha,\alpha_b) &= (\frac{1}{2}+\cos^2\alpha)(\alpha-\alpha_b) + \frac{1}{4}(\sin 2\alpha - \sin 2\alpha_b) \\
&\quad -2\cos\alpha(\sin\alpha - \sin\alpha_b)\,, \\
X3(\alpha_{a1},\alpha_{a2}) &= \rho(\sin\alpha_{a2} - \sin\alpha_{a1}) - \cos\alpha(\alpha_{a2}-\alpha_{a1})\,,
\end{aligned}
\tag{5}
$$

α_b – the angle determining the depth of the plastifying zone of the concrete,
α_{a1} – the angle determining the depth of the plastifying zone of the compressive steel,
α_{a2} – the angle determining the depth of the plastifying zone of the tensile steel,
t – the thickness of the cross-section $t = R - r$,
μ – the ratio of areas, steel to concrete.

The equilibrium equation of the bending moments in the section under consideration takes in turn the following form:

$$
\begin{aligned}
&-\frac{1}{2}\frac{1-\mu}{\gamma_c}(\sin\alpha_b - \sin\alpha_1) + \frac{1}{2}\frac{1-\mu}{\gamma_c}\frac{\dot{\epsilon}}{\rho_R - \cos\alpha}\Bigg[Y_1(\alpha,\alpha_b) \\
&+\frac{\dot{\epsilon}}{4(\rho_R - \cos\alpha)}Y_2(\alpha,\alpha_b)\Bigg] + \frac{1}{2}\mu\frac{f_{yk}}{f_{ck}}\Bigg[-\frac{1}{\gamma_s}\rho(\sin\alpha_{a1} - \sin\alpha_1) \\
&+\frac{1}{\epsilon_s}\frac{\dot{\epsilon}}{\rho_R - \cos\alpha}Y_3(\alpha_{a1},\alpha_{a2}) + \frac{1}{\gamma_s}\rho(\sin\alpha_2 - \sin\alpha_{a2})\Bigg] \\
&+\frac{M}{4r_m^2 t f_{ck}} = 0\,,
\end{aligned}
\tag{6}
$$

where:

$$
\begin{aligned}
Y_1(\alpha,\alpha_b) &= \frac{1}{2}(\alpha-\alpha_b) + \frac{1}{4}(\sin 2\alpha - \sin 2\alpha_b) \\
&\quad - \cos\alpha(\sin\alpha - \sin\alpha_b)\,, \\
Y_2(\alpha,\alpha_b) &= (1+\cos^2\alpha)(\sin\alpha - \sin\alpha_b) - \frac{1}{3}(\sin^3\alpha - \sin^3\alpha_b) \\
&\quad - \cos\alpha\left[\alpha - \alpha_b + \frac{1}{2}(\sin 2\alpha - \sin 2\alpha_b)\right]\,, \\
Y_3(\alpha_{a1},\alpha_{a2}) &= \rho\left\{\rho\left[\frac{1}{2}(\alpha_{a2}-\alpha_{a1}) + \frac{1}{4}(\sin 2\alpha_{a2} - \sin 2\alpha_{a1})\right]\right. \\
&\quad \left. - \cos\alpha(\sin\alpha_{a2} - \sin\alpha_{a1})\right\}\,.
\end{aligned}
\tag{7}
$$

The equations (4)-(7) describe all of the eight possible cases (schemes) of behaviour of the section under consideration. Let us consider the case when both concrete and steel are in plastic phase. The conditions of the strain continuity for the concrete and the compressive and tensile steels are expressed, respectively:

$$\frac{\cos\alpha_b - \cos\alpha}{\rho_R - \cos\alpha}\,\dot{\epsilon} = -2\,, \tag{8}$$

$$\frac{\rho\cos\alpha_{a1} - \cos\alpha}{\rho_R - \cos\alpha}\,\dot{\epsilon} = -\frac{\epsilon_s}{\gamma_s}\,, \tag{9}$$

$$\frac{\rho\cos\alpha_{a2} - \cos\alpha}{\rho_R - \cos\alpha}\,\dot{\epsilon} = \frac{\epsilon_s}{\gamma_s}\,. \tag{10}$$

Thus, the problem is described by the set of the five nonlinear equations given in the form (4), (6), (8)-(10) with the unknown variables α, $\dot{\epsilon}$, α_b, α_{a1}, α_{a2}.

3. DESCRIPTION OF THE OPTIMIZATION ALGORITHM USED FOR SOLVING THE SETS OF THE DERIVED EQUATIONS

3.1. FORMULATION OF THE PROBLEM

The purpose of the paper is to solve the derived set of nonlinear equations of the form

$$F_i(\boldsymbol{x}) = 0, \qquad i = 1, \ldots, n\,. \tag{11}$$

Number of equations is equal to the number of unknown variables in any problem considered in our paper. Although this number is different depending on the states of the steel and concrete.

Formulating the optimization problem the authors have decided to minimize the sum of second powers of the F_i functions, i.e. the resulting optimization problem is as follows

$$\begin{array}{ll} \min_{\boldsymbol{x}\in R^n} & f(\boldsymbol{x}) = \sum_{i=1}^{n} F_i^2(\boldsymbol{x})\,, \\ \text{s.t.} & x_i^L \le x_i \le x_i^U, \qquad i = 1, \ldots, n\,. \end{array} \tag{12}$$

Box constraints in the problem follow from the mechanical interpretation of the unknowns. Functions F_i are nonlinear and therefore the optimization problem is also nonlinear. The problem has got some unpleasant numerical properties. The minimized functions are very flat in the major part of the feasible region.

The authors have used three solvers developed ourselves in the standard *ANSI C* language. The first two use the least squares reformulation of the problem and apply the unconstrained optimization methods to solve. First of them implements the local BFGS quasi-Newton minimizer and the second the Hooke-Jeeves direct search method.

Although the BFGS and Hooke-Jeeves methods are the unconstrained optimization methods, in this implementation, box constraints on the parameters have been introduced and the algorithm rules have been modified appropriately to ensure feasibility (see section 3.2). For comparison purposes the nongradient routine implementing the modified Hook-Jeeves method has been prepared. Its description may be found for instance in Bazaraa et al [1], Fletcher [5]).

The third solver executes iterations aiming to solve directly the set of nonlinear equations (11).

3.2. BFGS QUASI-NEWTON LOCAL MINIMIZATION METHOD

The authors have realized a variant of the BFGS method. It belongs to the class of the so-called quasi-Newton methods (see for instance Bazaraa et al [1], Bertsekas [2], Fletcher [5], Goldfarb [6] or Stachurski and Wierzbicki [9]). The BFGS method starts from a given starting point x^0 and realizes typical for gradient unconstrained optimization steps of the form

$$\boldsymbol{x}^{k+1} = \boldsymbol{x}^k + \tau^k * \boldsymbol{d}^k, \tag{13}$$

where $\boldsymbol{d}^k = -\boldsymbol{H}^k \nabla f(\boldsymbol{x}^k)$ is the search direction and τ^k is the stepsize coefficient selected in the directional minimization function. It utilizes the gradient and independent variables differences to update the approximation $\boldsymbol{H}^k$ of the inverse of the second order derivative $\left(\nabla^2 f(\boldsymbol{x}^k)\right)^{-1}$ of the minimized function according to the following formula

$$\begin{aligned} \boldsymbol{H}^{k+1} &= \boldsymbol{H}^k + \left(1 + \frac{\left(\boldsymbol{r}^k\right)^T \boldsymbol{H}^k \boldsymbol{r}^k}{\left(\boldsymbol{r}^k\right)^T \boldsymbol{s}^k}\right) \frac{\boldsymbol{s}^k \left(\boldsymbol{s}^k\right)^T}{\left(\boldsymbol{r}^k\right)^T \boldsymbol{s}^k} \\ &\quad - \frac{\boldsymbol{s}^k \left(\boldsymbol{r}^k\right)^T \boldsymbol{H}^k + \boldsymbol{H}^k \boldsymbol{r}^k \left(\boldsymbol{s}^k\right)^T}{\left(\boldsymbol{r}^k\right)^T \boldsymbol{s}^k}, \end{aligned} \tag{14}$$

where $\boldsymbol{r}^k = \boldsymbol{p}^{k+1} - \boldsymbol{p}^k$, $\boldsymbol{s}^k = \boldsymbol{x}^{k+1} - \boldsymbol{x}^k$ and $\boldsymbol{p}^k = \nabla f(\boldsymbol{x}^k)$.

Iterations of the local minimizer are stopped when the norm of the gradient (derivative) of function f is smaller than a given accuracy $\epsilon_{BFGS} > 0$.

Two variants of the directional minimization have been tested. In the first one, the successive quadratic/cubic approximations of function $\bar{f}(\tau) = f(\boldsymbol{x}^k + \tau * \boldsymbol{d}^k)$ have been used. Search along the direction is stopped, when the following step-size rule (it is referred later as "the Wolfe-Powell step-size rule" assuming the name used by Fletcher [5]) is satisfied, i.e.

$$\frac{|d\bar{f}(\tau^k)|}{-d\bar{f}(0)} = \frac{|(\nabla f(\boldsymbol{x}^k + \tau^k \boldsymbol{d}^k))^T \boldsymbol{d}^k|}{-(\nabla f(\boldsymbol{x}^k))^T \boldsymbol{d}^k} \le \omega, \qquad \text{for some} \quad \omega \in (0,1)\,. \tag{15}$$

Parameters ϵ_{BFGS} and ω are specified by the user.

The choice of the quadratic or cubic approximation depends on the relation between between the value of $\bar{f}(\tau)$ at some trial point τ and the corresponding value of the linearization at build in the the left bound τ_L, i.e.

- Cubic if

$$\bar{f}(\tau) < \bar{f}(\tau_{\mathrm{L}}) + (1+\theta)\tau\bar{f}'(\tau_{\mathrm{L}})\,. \tag{16}$$

- Bisection if

$$\bar{f}(\tau_{\mathrm{L}}) + (1+\theta)\tau\bar{f}'(\tau_{\mathrm{L}}) \le \bar{f}(\tau) \le \bar{f}(\tau_{\mathrm{L}}) + (1-\theta)\tau\bar{f}'(\tau_{\mathrm{L}})\,. \tag{17}$$

- Quadratic approximation if

$$\bar{f}(\tau) > \bar{f}(\tau_{\mathrm{L}}) + (1-\theta)\tau\bar{f}'(\tau_{\mathrm{L}})\,. \tag{18}$$

The constant parameter θ belongs to the interval $(0, 1)$.

Those conditions represent the idea that for τ close to τ_L positive curvature suggests the use of quadratic approximation, while the negative one the cubic approximation. The third intermediate case reflects the situation when $\bar{f}$ is locally close to linear.

The second directional minimization tested assumed start from a given step-length and its consecutive decrease via a user specified coefficient. The first point satisfying the second Goldstein test (see Goldstein [7])

$$f(\boldsymbol{x}^k + \tau^k\boldsymbol{d}^k) - f(\boldsymbol{x}^k) \le \varrho\tau^k\nabla f(\boldsymbol{x}^k)^T\boldsymbol{d}^k \tag{19}$$

is accepted as the result of the directional minimization ($\varrho \in (0, \frac{1}{2})$.

This general scheme of the minimizer has been modified to take into account box constraints on variables. This is in accordance with the modern optimization routines which are usually implemented so that they minimize a function subject to box constraints, i.e. solve the problem

$$\begin{aligned} &\min\nolimits_{\boldsymbol{x}\in R^n} \quad f(\boldsymbol{x})\,,\\ &\text{s.t.} \qquad x_i^L \le x_i \le x_i^U\,, \qquad \text{for } i = 1,\dots,n. \end{aligned} \tag{20}$$

It was also necessary to modify the stopping criterion. The Kuhn-Tucker necessary optimality conditions in the case of box constraints take the form

(1) the following inequalities should be satisfied on the boundaries

$$\begin{aligned} &\text{if} \quad x_i^{k+1} = x_i^L \quad \text{then} \quad p_i^{k+1} \ge 0\,,\\ &\text{if} \quad x_i^{k+1} = x_i^U \quad \text{then} \quad p_i^{k+1} \le 0\,,\\ &\text{for} \quad i = 1,\dots,n\,, \end{aligned}$$

where $\boldsymbol{p}^{k+1} = \nabla f(\boldsymbol{x}^{k+1})$.

(2) the norm of the gradient in the subspace of variables that are not on their bounds in the new point $\boldsymbol{x}^{k+1}$ should be equal to 0. Of course, in practice it is verified, whether it is sufficiently small.

The resulting algorithm is as follows:

0. Specify bounds x^L and x^U on variables. Select a feasible starting point x^0 satisfying the box constraints. Choose accuracy parameters – $\epsilon_{BFGS} > 0$, $\omega \in (0,1)$. Calculate values of gradient p^0 and function f^0 at the starting point x^0. Take $H^0 = I$, where I is the identity matrix, $k := 0$.
1. Calculate the current search direction according to the following formula
$$d^k = -H^k p^k \,.$$
2. Find $\tau \leq 0$ such that the Wolfe-Powell step-size rule is satisfied, i.e.
$$\frac{|(\nabla f(x^k + \tau^k d^k))^T d^k|}{-(\nabla f(x^k))^T d^k} \leq \omega \,.$$
3. Calculate the next point
$$x^{k+1} = x^k + \tau^k d^k \,,$$
and the gradient at the new point p^{k+1}.
4. Check the stopping criterion (the Kuhn-Tucker conditions). If the stopping criteria are satisfied then STOP.
5. Compute the gradient $r^k = p^{k+1} - p^k$ and independent variables $s^k = x^{k+1} - x^k$ differences. Update the approximation of the inverse Hessian using formula (14).
6. Set $x^{k+1} = x^k$, $p^{k+1} = p^k$. Increase the iteration index k by one. Calculate $f(x^k)$. Return to Step 1.

Directional minimization implemented in Step 2. is not typical. In fact, the function $\bar{f}(P(x^k + \tau d^k))$ is minimized instead of $\bar{f}(x^k + \tau d^k)$, where P represents the projection operator on the set of feasible points defined by the box constraint. So this means that the inverse Hessian approximation in the whole space is maintained, the descent direction in the whole space is generated and the directional minimization is carried out in a specific way. It differentiates substantially this approach from the typical active set methods for problems with linear constraints.

3.3. THE HOOKE-JEEVES DIRECT SEARCH METHOD

The Hooke-Jeeves method (see, for instance Hooke and Jeeves (1961), Findeisen at al. (1977), Stachurski and Wierzbicki (1999)) represents the class of an ad hoc direct approach to the minimization of the n-dimensional function. It makes use of n mutually orthogonal search vectors forming a basis of the R^n space. Two kinds of steps are considered. First, we fix a basic point. Starting from the basic point we move either forward or back with the fixed step-size τ along the consecutive basis vectors. Afterwards, if we succeed we have got new point with smaller value of the minimized function. In the case of success we try to go further along the vector joining the new point with the basic one. In the case of failure the step-size τ is decreased by a constant coefficient. The whole process is repeated untill τ is larger than the given accuracy.

The algorithm is as follows.

Initialization. Select $\boldsymbol{x}^0$ - starting point, $\left[\boldsymbol{d}^1, \dots, \boldsymbol{d}^n\right]$ - basis formed by the n mutually orthogonal vectors (n - number of independent variables), τ - starting step-size length, $\beta \in (0,1)$ - step-length reduction coefficient, ϵ - accuracy parameter. Set the iteration counter to zero $k := 0$, calculate $f^0 = f(\boldsymbol{x}^0)$.

Trial Step.
Set $\boldsymbol{x}_B = x^k$, $f_B = f^k$.
For $i = 0, \dots, n$ execute the trial step
Calculate $\boldsymbol{x}^i = \boldsymbol{x}^k + \tau \boldsymbol{d}^i$, $f^i = f(\boldsymbol{x}^i)$.
If $f^i < f^k$ then $\boldsymbol{x}^{k+1} = \boldsymbol{x}^i$, $f^{k+1} = f^i$
otherwise
calculate $\boldsymbol{x}^i = \boldsymbol{x}^k - \tau \boldsymbol{d}^K$, $f^i = f(\boldsymbol{x}^i)$.
If $f^i < f^k$ then $\boldsymbol{x}^{k+1} = \boldsymbol{x}^i$, $f^{k+1} = f^i$
If $i \leq n$ then $k := k+1$, return to the beginning to the loop otherwise go to the Acceleration Step.

Acceleration Step.
If $f_B \leq f^k$ then

- if $\tau < \epsilon$ then STOP, assume that $\boldsymbol{x}^k$ as the optimal solution
- decrease the step-length $\tau = \beta\tau$ and return to Step 1

otherwise
Calculate $\boldsymbol{x}^i = \boldsymbol{x}^k + \left(\boldsymbol{x}^k - \boldsymbol{x}_B\right)$, $f^i = f(\boldsymbol{x}^i)$.
If $f^i < f_B$ then $\boldsymbol{x}_B = \boldsymbol{x}^{k+1} = \boldsymbol{x}^i$, $f_B = f^{k+1} = f^i$
otherwise
$\boldsymbol{x}_B = \boldsymbol{x}^k$, $f_B = f^k$.
Increase the iteration counter $k := k+1$ and return to Step 1.

3.4. BROYDEN'S QUASI-NEWTON METHOD

Broyden's method for solving sets of nonlinear equations is similar to the BFGS foreseen for unconstrained optimization. It uses iterations of the following form

$$\boldsymbol{x}^{k+1} = \boldsymbol{x}^k + \boldsymbol{d}^k \,, \tag{21}$$

where step $\boldsymbol{d}^k$ is the solution of the following set of linear equations

$$\boldsymbol{B}^k \boldsymbol{d}^k = -\boldsymbol{F}(\boldsymbol{x}^k)\,. \tag{22}$$

Matrix $\boldsymbol{B}^k$ is updated at each iteration similarly as in the BFGS method. The important difference is that those matrices are not necessarily symmetric. The Jacobi matrix approximated by $\boldsymbol{B}^k$ is usually not symmetric while the Hessian in the optimization problems is symmetric.

The updated $\boldsymbol{B}^{k+1}$ should fulfill the quasi-Newton condition

$$\boldsymbol{B}^{k+1}\boldsymbol{s}^k = \boldsymbol{y}^k \,, \tag{23}$$

where $\boldsymbol{s}^k = \boldsymbol{x}^{k+1} - \boldsymbol{x}^k$ and $\boldsymbol{r}^k = \boldsymbol{F}^{k+1} - \boldsymbol{F}^k$. It reflects the approximate equality held by the Jacobi matrix

$$\boldsymbol{F}(\boldsymbol{x}^k) = \boldsymbol{F}^{k+1} + \boldsymbol{J}(\boldsymbol{x}^{k+1})\left(\boldsymbol{x}^k - \boldsymbol{x}^{k+1}\right) \,, \tag{24}$$

or equivalently

$$\boldsymbol{r}^k = \boldsymbol{J}(\boldsymbol{x}^{k+1})\boldsymbol{s}^k \,. \tag{25}$$

Now let us impose on $\boldsymbol{B}^{k+1}$ two requirements: 1 - image on vectors orthogonal to $\boldsymbol{s}^k$ is the same as of $\boldsymbol{B}^k$, 2 - the quasi-Newton condition helds.

Those requirements are verified by the following update

$$\boldsymbol{B}^{k+1} = \boldsymbol{B}^k + \frac{\left(\boldsymbol{r}^k - \boldsymbol{B}^k\boldsymbol{s}^k\right)(\boldsymbol{s}^k)^T}{(\boldsymbol{s}^k)^T\boldsymbol{s}^k} \,. \tag{26}$$

The Broyden method described above is often implemented so that the equation (22) is solved directly at each step by means of the Gauss elimination. In the authors' opinion it is an unnecessary loss of computational effort. Therefore the corresponding updating formula for the inverse of $\boldsymbol{B}^k$ has been derived using the Householder formula

$$\boldsymbol{H}^{k+1} = \boldsymbol{H}^k - \frac{\left(\boldsymbol{H}^k\boldsymbol{r}^k - \boldsymbol{s}^k\right)(\boldsymbol{s}^k)^T\boldsymbol{H}^k}{(\boldsymbol{s}^k)^T\boldsymbol{H}^k\boldsymbol{r}^k} \,. \tag{27}$$

It is easy to verify that $\boldsymbol{H}^{k+1}$ is the inverse of $\boldsymbol{B}^{k+1}$. See Lemma 1 below.

Lemma 3.1. *Let $\boldsymbol{B}^k$ be an $n \times n$ nonsingular square matrix and $\boldsymbol{H}^k$ be its inverse. Let furthermore the coefficient $(\boldsymbol{s}^k)^T\boldsymbol{H}^k\boldsymbol{r}^k \neq 0$ assumes nonzero value.*

Then $\boldsymbol{H}^{k+1}$ and $\boldsymbol{B}^{k+1}$ generated by formulae (27) and (26) verify the equality

$$\boldsymbol{H}^{k+1}\boldsymbol{B}^{k+1} = \boldsymbol{I} \,,$$

i.e. $\boldsymbol{H}^{k+1}$ is the inverse of $\boldsymbol{B}^{k+1}$.

Proof. Direct calculations show the desired thesis

$$\boldsymbol{H}^{k+1}\boldsymbol{B}^{k+1} = \left[\boldsymbol{H}^k - \frac{\left(\boldsymbol{H}^k\boldsymbol{r}^k - \boldsymbol{s}^k\right)(\boldsymbol{s}^k)^T\boldsymbol{H}^k}{(\boldsymbol{s}^k)^T\boldsymbol{H}^k\boldsymbol{r}^k}\right]\left[\boldsymbol{B}^k + \frac{\left(\boldsymbol{r}^k - \boldsymbol{B}^k\boldsymbol{s}^k\right)(\boldsymbol{s}^k)^T}{(\boldsymbol{s}^k)^T\boldsymbol{s}^k}\right]$$

$$= \boldsymbol{H}^k\boldsymbol{B}^k + \frac{\left(\boldsymbol{H}^k\boldsymbol{r}^k - \boldsymbol{H}^k\boldsymbol{B}^k\boldsymbol{s}^k\right)(\boldsymbol{s}^k)^T}{(\boldsymbol{s}^k)^T\boldsymbol{s}^k} - \frac{\left(\boldsymbol{H}^k\boldsymbol{r}^k - \boldsymbol{s}^k\right)(\boldsymbol{s}^k)^T\boldsymbol{H}^k\boldsymbol{B}^k}{(\boldsymbol{s}^k)^T\boldsymbol{H}^k\boldsymbol{r}^k}$$

$$- \frac{\left(\boldsymbol{H}^k\boldsymbol{r}^k - \boldsymbol{s}^k\right)(\boldsymbol{s}^k)^T\boldsymbol{H}^k}{(\boldsymbol{s}^k)^T\boldsymbol{H}^k\boldsymbol{r}^k}\frac{\left(\boldsymbol{r}^k - \boldsymbol{B}^k\boldsymbol{s}^k\right)(\boldsymbol{s}^k)^T}{(\boldsymbol{s}^k)^T\boldsymbol{s}^k}$$

$$= \boldsymbol{I} + \frac{\left(\boldsymbol{H}^k\boldsymbol{r}^k - \boldsymbol{s}^k\right)(\boldsymbol{s}^k)^T}{(\boldsymbol{s}^k)^T\boldsymbol{s}^k} - \frac{\left(\boldsymbol{H}^k\boldsymbol{r}^k - \boldsymbol{s}^k\right)(\boldsymbol{s}^k)^T}{(\boldsymbol{s}^k)^T\boldsymbol{H}^k\boldsymbol{r}^k}$$

$$- \frac{\left(\boldsymbol{H}^k\boldsymbol{r}^k - \boldsymbol{s}^k\right)(\boldsymbol{s}^k)^T\left((\boldsymbol{s}^k)^T\boldsymbol{H}^k\boldsymbol{r}^k - (\boldsymbol{s}^k)^T\boldsymbol{s}^k\right)}{(\boldsymbol{s}^k)^T\boldsymbol{H}^k\boldsymbol{r}^k \cdot (\boldsymbol{s}^k)^T\boldsymbol{s}^k}$$

$$= \boldsymbol{I} + \left(\boldsymbol{H}^k\boldsymbol{r}^k - \boldsymbol{s}^k\right)(\boldsymbol{s}^k)^T$$

$$\times \frac{\left((\boldsymbol{s}^k)^T\boldsymbol{H}^k\boldsymbol{r}^k - (\boldsymbol{s}^k)^T\boldsymbol{s}^k\right) - \left((\boldsymbol{s}^k)^T\boldsymbol{H}^k\boldsymbol{r}^k - (\boldsymbol{s}^k)^T\boldsymbol{s}^k\right)}{(\boldsymbol{s}^k)^T\boldsymbol{H}^k\boldsymbol{r}^k \cdot (\boldsymbol{s}^k)^T\boldsymbol{s}^k}. \quad \square$$

The resulting algorithm is presented below

0. Select a feasible starting point x^0 satisfying the box constraints. Choose accuracy parameters – ϵ_{Br}, ϵ_h, $\epsilon_{H\,Update}$, where: ϵ_{Br} – accuracy coefficient in the residua stopping criterion, ϵ_h – step in the starting Inverse Jacobian evaluation and $\epsilon_{H\,Update}$ – accuracy parameter used in the safeguard criterion ensuring nonsingularity of the new update. Calculate values of equations functions F^0 at the starting point $\boldsymbol{x}^0$. Select $\boldsymbol{H}^0 = \boldsymbol{I}$, where $\boldsymbol{I}$ is the identity matrix, $k := 0$.

   Calculate n equations functions values $\boldsymbol{F}_i = \boldsymbol{F}(\boldsymbol{x}_i)$ at points $\boldsymbol{x}_i = \boldsymbol{x}^0 + \epsilon_h\boldsymbol{e}_i$, where $\boldsymbol{e}_i$ denotes the i–th versor of the cartesian coordinates. Compute new $\boldsymbol{H}^0$ appying n times updating formula (27) with pairs of verctors $\boldsymbol{s}_i = \boldsymbol{x}_i - \boldsymbol{x}^0$, $\boldsymbol{r}_i = \boldsymbol{F}_i - \boldsymbol{F}^0$.
1. Calculate the current search direction according to the following formula

$$\boldsymbol{d}^k = -\boldsymbol{H}^k\boldsymbol{F}^k\,.$$

2. Calculate the next point

$$\boldsymbol{x}^{k+1} = \boldsymbol{x}^k + \boldsymbol{d}^k$$

and the vector of equations functions values at the new point $\boldsymbol{F}^{k+1}$.

3. Check the stopping criterion, i.e. verify if the following condition

$$res = \sqrt{\sum_{i=0}^{n} F_i^2(\boldsymbol{x}^{k+1})} < \epsilon_{Br} \, . \tag{28}$$

If the stopping criterion is satisfied satisfied then STOP.

4. Compute the vector of the residua differences $\boldsymbol{r}^k = \boldsymbol{F}^{k+1} - \boldsymbol{F}^k$ and independent variables $\boldsymbol{s}^k = \boldsymbol{x}^{k+1} - \boldsymbol{x}^k$ differences. Verify the nonsingularity test of $\boldsymbol{H}^{k+1}$.

   If

$$(\boldsymbol{s}^k)^T \boldsymbol{H}^k \boldsymbol{r}^k > \epsilon_{H\,Update}$$

update the approximation of the inverse Jacobian using formula (27).

5. Set $\boldsymbol{x}^{k+1} = \boldsymbol{x}^k$, $\boldsymbol{F}^{k+1} = \boldsymbol{F}^k$. Increase the iteration index k by one. Return to Step 1.

Closer look at algorithm shows that the starting $\boldsymbol{H}^0$ is calculated applying small increments in the neighbourhood of the point $\boldsymbol{x}^0$ and using the same updating scheme as in normal steps. The aim is to start with the approximation $\boldsymbol{H}^0$ close to the Jacobian inverse $\boldsymbol{J}^{-1}(\boldsymbol{x}^0)$.

4. NUMERICAL EXAMPLES

The presented approach enables the determination of strains and stresses in the sections under consideration by the interactive analysis. There are eight possible cases (schemes) of behaviour of the section under consideration. The problem is described mathematically by a set of equations which are nonlinear and difficult to be solved. Every behaviour scheme results in a different set of equations. It is not known a priori which is the correct one. Therefore one has to start with the simplest possible scheme (both steel and concrete are elastic) and verify some conditions which indicate the next scheme and the corresponding set of nonlinear equations to be tried.

The set of the nonlinear equations given in the form (4)-(10) is solved directly by means of the Broyden secant method and alternatively using the least squares approach. In the second one the problem is reformulated and assumes the form of an optimization problem. In fact, the sum of the second powers of their residuals is minimized. The resulting optimization problems have been solved by means of the modified BFGS quasi-Newton and/or Hooke-Jeeves direct search methods.

In the selected example the yield stress of steel is assumed as $f_{yk} = 410\,\mathrm{MPa}$, partial safety factor for steel $\gamma_s = 1.15$, the characteristic strength of concrete in compression $f_{ck} = 20\,\mathrm{MPa}$, partial safety factor for concrete $\gamma_c = 1.5$. The structure is subject to the normal force $N = 16900\mathrm{kN}$ and the bending moment $M = N \cdot e$, where e is the eccentricity of the force

N. The geometry of the section is described by the following parameters: outer radius $R = 4.8$m, inter radius $r = 4.3$m, the reference radius of steel $r_s = 4.76$m, $\alpha_2 = \pi$ (i.e. the second opening is missing), the ratio of areas (steel/concrete) $\mu = 1.0\%$. Both the closed section and the ones weakened by one opening of three different sizes were considered. Solutions corresponding to different values of the eccentricity ratio (e/R) were searched.

The problem has created serious numerical difficulties. Hence the computational time was not as important from the authors point of view as to reach the solution with the desired accuracy. It was relatively easy to solve the set of equations corresponding to elastic behaviour of both material components (concrete, steel). However even in this case the least squares methods sometimes required careful selection of the starting point. The Broyden method has usually converged very fast from the assumed default starting point.

When one or two of the material components were assumed to be in the plastic state the corresponding sets of nonlinear equations were sometimes very hard to solve. The Broyden secant method has usually found a solution which was not physically acceptable (calculated values were outside the feasible scope, not permitted from the physical point of view), as for instance for: $e/R = 10.08$, $\alpha_1 = 0.384$, steel is in the plastic state, concrete remains elastic. Broyden's method started from the default starting point gave the following answer:

$$\alpha = -2.108, \quad \epsilon = -6.744, \quad \alpha_{s2} = -34.721, \quad res = 6.3 \cdot 10^{-11}$$

Both angles α and α_{s2} are outside their feasible scope $[0, \pi]$.

The BFGS and Hook-Jeeves methods were often not able to find the solution with the desired accuracy at all, as for instance: $e/R = 12.0$, $\alpha_1 = 0.384$, steel is in plastic state, concrete remains elastic. BFGS method started from the default starting point returned the point with the residuals norm $res = 0.428$ and the Hook-Jeeves method with $res = 3.15 \cdot 10^{-4}$.

After many runs of the program the most successful strategy has been found - first start from the default starting point, then continue with the Hook-Jeeves method starting from the approximate solution found by the BFGS and as the final move - run the Broyden method from the solution found by the previously applied method. The program implemented in the standard *ANSI C* progarmming language is prepared so that it permits smoothly switch from one method to another without changing the model and keeping the best point from the previous run as the starting for the current. This procedure is very well illustrated by the calculations for the closed ring section with the large eccentricity ratio $e/R = 15.36$ $(e = 3.5)$. It is depicted graphically in Diagram 1.

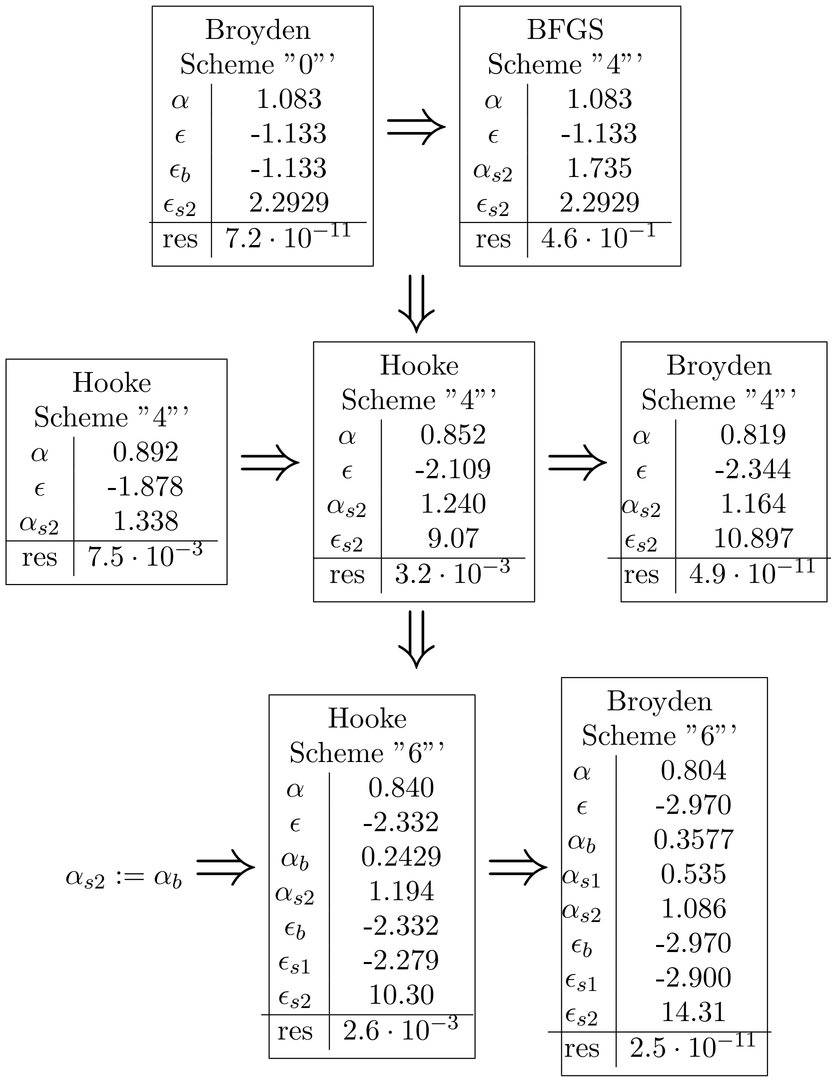

Diagram 1: Schedule of calculations for the closed ring section when both steel and concrete has plastified

The results of the numerical experiment are summarized in Tables 1, 2, 3 and 4. Table 1 contains results for the closed ring section. Other three tables summarize calculations for the ring sections with openings of different size characterized by different values of the angle α_1, Table 2 for $\alpha_1 = 0.192(11^0)$, Table 3 for $\alpha_1 = 0.384(22^0)$ and Table 4 for $\alpha_1 = 0.576(33^0)$. Each table contains values computed for a sequence of the increasing eccentricity ratios. Final values of all unknown variables, some indicators important from the engineer point of view and the final norm of the residuals are notified for every particular ratio. The solutions were accepted when the minimized sum of the second powers of the residua was smaller than 10^{-10} and rejected otherwise. The point of switching the calculations from one scheme to another are also notified.

e/R	α	ϵ	ϵ_S	res
2.88	2.609	-0.198	0.019	$4.7 \cdot 10^{-14}$
3.36	2.189	-0.221	0.063	$4.3 \cdot 10^{-15}$
3.84	1.746	-0.329	0.221	$6.4 \cdot 10^{-10}$
4.32	1.583	-0.379	0.372	$9.0 \cdot 10^{-11}$
4.80	1.421	-0.432	0.548	$1.9 \cdot 10^{-11}$
5.28	1.329	-0.485	0.737	$3.3 \cdot 10^{-11}$
5.76	1.262	-0.538	0.934	$4.0 \cdot 10^{-11}$
7.20	1.287	-0.468	0.802	$9.3 \cdot 10^{-12}$
8.40	1.223	-0.547	1.063	$1.0 \cdot 10^{-12}$
9.60	1.180	-0.627	1.326	$6.7 \cdot 10^{-11}$
10.08	1.167	-0.659	1.432	$2.4 \cdot 10^{-12}$
10.80	1.150	-0.708	1.591	$7.4 \cdot 10^{-11}$
12.0	1.128	-0.789	1.857	$8.2 \cdot 10^{-12}$

Steel has switched to the plastic state because $\epsilon_S > \epsilon_{Gr} = 1.697$. Concrete remains elastic.

e/R	α	ϵ	α_{s2}	ϵ_S	res
13.2	1.170	-0.910	2.518	1.967	$2.6 \cdot 10^{-13}$
13.92	1.136	-1.004	2.243	2.322	$3.9 \cdot 10^{-13}$
15.36	0.819	-2.344	1.164	10.897	$4.9 \cdot 10^{-11}$

Concrete has plastified.

e/R	α	ϵ	α_b	α_{s1}	α_{s2}	ϵ_S	res
15.36	0.804	-2.97	0.3677	0.535	1.086	14.31	$2.5 \cdot 10^{-11}$

TABLE 1. Results for the ring section without openings

e/R	α	ϵ	ϵ_S	res
4.8	1.604	-0.396	0.369	$4.4 \cdot 10^{-12}$
7.2	1.361	-0.599	0.888	$3.0 \cdot 10^{-11}$
8.4	1.357	-0.702	1.156	$8.9 \cdot 10^{-12}$
9.6	1.271	-0.807	1.426	$4.0 \cdot 10^{-12}$
10.08	1.259	-0.849	1.535	$4.0 \cdot 10^{-11}$
10.80	1.245	-0.913	1.638	$2.9 \cdot 10^{-12}$
12.0	1.226	-1.022	1.972	$1.4 \cdot 10^{-11}$
7.20	1.287	-0.468	0.802	$9.3 \cdot 10^{-12}$
8.40	1.223	-0.547	1.063	$1.0 \cdot 10^{-12}$
9.60	1.180	-0.627	1.326	$6.7 \cdot 10^{-11}$
10.08	1.167	-0.659	1.432	$2.4 \cdot 10^{-12}$
10.80	1.150	-0.708	1.591	$7.4 \cdot 10^{-11}$
12.0	1.226	-1.022	1.972	$1.4 \cdot 10^{-11}$

Steel has switched to the plastic state because $\epsilon_S > \epsilon_{Gr} = 1.697$. Concrete remains elastic.

e/R	α	ϵ	α_{s2}	ϵ_S	res
12.0	1.273	-1.048	2.689	1.842	$1.9 \cdot 10^{-13}$
13.2	1.220	-1.250	2.208	2.443	$4.6 \cdot 10^{-13}$
13.92	1.170	-1.441	1.955	3.114	$3.8 \cdot 10^{-11}$

TABLE 2. Results for the ring section with a single opening $\alpha_1 = 0.192(11^0)$

Values of the stresses in the concrete σ_b and in the steel σ_s in the closed ring section are plotted directly as a function of the eccentricity ratio e/R and the size of the opening $2\alpha_1$ (depicted on Figure 3 and 4). The presented curves indicate that the obtained relationships reflect the physical nonlinearity of the concrete and steel.

5. CONCLUSIONS

The following conclusions can be deduced:

(1) The implemented modified BFGS, Hook-Jeeves and Broyden quasi-Newton methods have been successfully used to solve the sets of equations proposed for determining and analysis of stresses in the RC ring cross sections weakened by openings. The computational experiment points that the most successfull strategy is to start calculations with the BFGS, followed by the Hook-Jeeves (used sometimes several times) and apply Broyden method at the final stage to obtain good numerical accuracy. It refers especially to the inelastic cases.

e/R	α	ϵ	ϵ_S	res
4.8	1.627	-0.534	0.475	$1.0 \cdot 10^{-12}$
7.2	1.442	-0.806	1.20	$8.3 \cdot 10^{-11}$
8.4	1.398	-0.947	1.305	$2.1 \cdot 10^{-12}$
9.6	1.369	-1.091	1.590	$6.5 \cdot 10^{-11}$
10.08	1.360	-1.150	1.707	$5.3 \cdot 10^{-12}$

Steel switches to the plastic state because $\epsilon_S > \epsilon_{Gr} = 1.697$. Concrete remains elastic.

e/R	α	ϵ	α_{s2}	ϵ_S	res
10.80	1.378	-1.262	2.760	1.807	$9.6 \cdot 10^{-11}$
12.0	1.326	-1.534	2.249	2.434	$9.4 \cdot 10^{-11}$
13.2	1.233	-2.082	1.820	3.966	$9.8 \cdot 10^{-11}$
13.92	1.149	-2.873	1.545	6.473	$1.8 \cdot 10^{-11}$

TABLE 3. Results for the ring section with a single opening $\alpha_1 = 0.384(22^0)$

e/R	α	ϵ	ϵ_S	res
4.8	1.666	-0.760	0.629	$1.5 \cdot 10^{-11}$
7.2	1.531	-1.146	1.227	$4.2 \cdot 10^{-11}$
8.4	1.498	-1.349	1.535	$2.81 \cdot 10^{-11}$
9.6	1.477	-1.559	1.847	$1.4 \cdot 10^{-14}$

Steel switches to the plastic state because $\epsilon_S > \epsilon_{Gr} = 1.697$. Concrete remains elastic.

e/R	α	ϵ	α_{s2}	ϵ_S	res
10.08	1.466	-1.726	2.488	2.088	$2.8 \cdot 10^{-13}$
10.80	1.425	-2.023	2.204	2.648	$6.2 \cdot 10^{-11}$
12.0	1.317	-3.149	1.746	5.080	$1.0 \cdot 10^{-10}$

TABLE 4. Results for the ring section with a single opening $\alpha_1 = 0.576(33^0)$

(2) Solutions with satisfactory accuracy were found in most cases encountered in engineering practice.
(3) The presented approach can be used for the design and dimensioning the RC structures having both open and closed ring cross sections.
(4) The obtained equations can be generalized for the section weakened by arbitrary number of openings located symmetrically in respect to the bending direction.

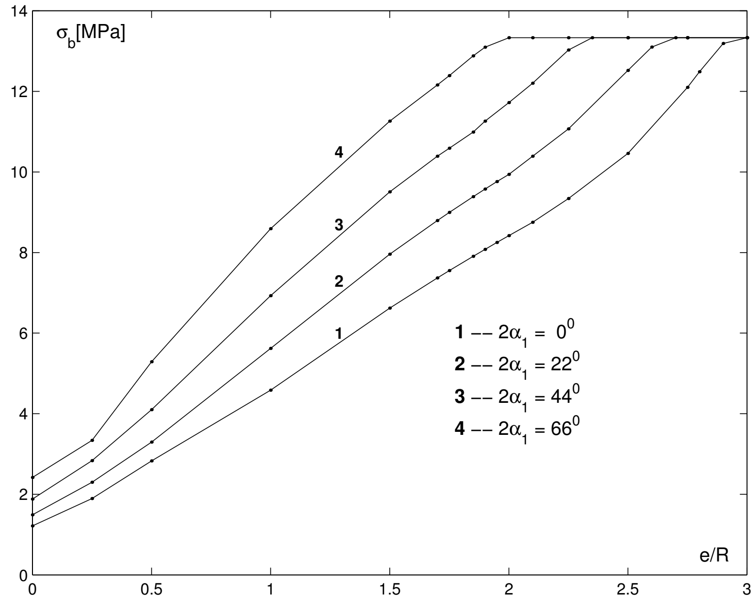

Figure 3. Stresses in concrete σ_b versus eccentricity ratio e/R and size of opening $2\alpha_1$

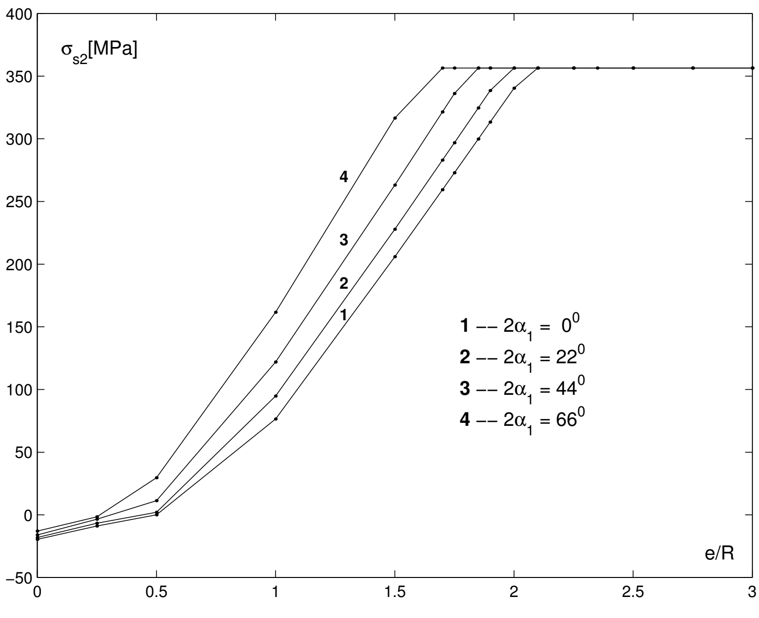

Figure 4. Tensile stresses in steel versus eccentricity ratio e/R and size of opening $2\alpha_1$

(5) The proposed model has got a very simple form of maximum five equations. Hence it creates a useful tool for practical design of the tower-like RC structures.

(6) The obtained formulas combined with the optimization methods are more suitable for the parametric study of such structure behavior than a sophisticated finite element package. The solution time is measured in seconds and therefore is negligible.

REFERENCES

[1] M.S. Bazaraa, J. Sherali, C.M. Shetty, *Nonlinear Programming. Theory and Algorithms*, John Wiley and Sons, New York, Chichester, Brisbane, Toronto, 1993.

[2] D.P. Bertsekas, *Nonlinear Programming*, Athena Scientific, Massachussets, 1997.

[3] C.G. Broyden, Quasi-Newton methods and their application to function minimikzation, *Mathematics of Computation*, **21** (1967), 368-381.

[4] C.G. Broyden, The convergence of a class of double rank minimization algorithms. Parts 1 and 2, *Journal of the Institute of Mathematics and its Applications*, **6** (1970), 76-90, 222-231.

[5] R. Fletcher, *Practical Methods of Optimization*, Second Edition, John Wiley and Sons, Chichester, 1987.

[6] D. Goldfarb, A family of variable metric methods derived by variational means, *Mathematics of Computation*, **24** (1982), 23-26.

[7] A.A. Goldstein, On steepest descent, *SIAM J. Control*, **3** (1965), 147-151.

[8] M. Lechman and A. Stachurski, Nonlinear section model for analysis of RC circular tower structures weakened by openings, *Structural Engineering and Mechanics*, **20** (2005), no. 2, 161-172.

[9] A. Stachurski and A.P. Wierzbicki, *Introduction to Optimization*, Second Edition, Podstawy Optymalizacji, in polish, Oficyna Wydawnicza Politechniki Warszawskiej, Warszawa, 2001.